



ELSEVIER

Contents lists available at ScienceDirect

## Thrombosis Research

journal homepage: [www.elsevier.com/locate/thromres](http://www.elsevier.com/locate/thromres)

## Full Length Article

# $\gamma$ D318Y fibrinogen shows no fibrin polymerization due to defective “A-a” and “B-b” interactions, whereas that of $\gamma$ K321E fibrinogen is nearly normal

Tomu Kamijo<sup>a</sup>, Saki Mukai<sup>b</sup>, Chiaki Taira<sup>a</sup>, Yumiko Higuchi<sup>a</sup>, Nobuo Okumura<sup>a,\*</sup><sup>a</sup> Department of Clinical Laboratory Investigation, Graduate School of Medicine, Shinshu University, Matsumoto, Japan<sup>b</sup> Department of Laboratory Medicine, Shinshu University Hospital, Matsumoto, Japan

## ARTICLE INFO

## Keywords:

Fibrinogen  
 $\beta$ -Module  
 $\gamma$ -Module  
 “A-a” interaction  
 “B-b” interaction  
 Dysfibrinogenemia

## ABSTRACT

**Background:** The fibrinogen  $\gamma$ -module has several functional sites and plays a role in dysfibrinogenemia, which is characterized by impaired fibrin polymerization. Variants, including  $\gamma$ D318Y and  $\gamma$  $\Delta$ N319D320, have been reported at the high affinity  $\text{Ca}^{2+}$ -binding site, and analyses using recombinant fibrinogen revealed the importance of this site for fibrinogen functions and secretion. We examined the polymerization abilities of the recombinant fibrinogen variants,  $\gamma$ D318Y and  $\gamma$ K321E.

**Materials and methods:**  $\gamma$ D318Y and  $\gamma$ K321E were produced using CHO cells and fibrinogen functions were examined using thrombin- or batroxobin-catalyzed polymerization, gel chromatography, protection against plasmin degradation, and factor XIIIa cross-linking.

**Results:**  $\gamma$ D318Y did not show any polymerization by thrombin or batroxobin, similar to  $\gamma$  $\Delta$ N319D320, whereas  $\gamma$ K321E had slightly impaired polymerization. The functions of  $\text{Ca}^{2+}$  binding, hole ‘a’, and the “D-D” interaction were markedly reduced in  $\gamma$ D318Y, and gel chromatography suggested altered protofibril formation. *In silico* analyses revealed that structural changes in the  $\gamma$ -module of these variants were inconsistent with polymerization results. The degree of structural changes in  $\gamma$ D318Y was moderate relative to those in  $\gamma$ D318A and  $\gamma$ D320A, which had markedly impaired polymerization, and  $\gamma$ K321E, which showed slightly impaired polymerization.

**Conclusion:** Our results suggest that no polymerization of  $\gamma$ D318Y or  $\gamma$  $\Delta$ N319D320 was due to the loss of both “A-a” and “B-b” interactions. Previous studies demonstrated that “B-b” interaction alone causes polymerization of neighboring  $\gamma$ D318A and  $\gamma$ D320A fibrinogen, which is subsequently decreased. Marked changes in the tertiary structure of the  $\gamma$ D318Y  $\gamma$ -module influenced the location and/or orientation of the adjacent  $\beta$ -module, which led to impaired “B-b” interactions.

## 1. Introduction

Fibrinogen is a 340-kDa plasma glycoprotein composed of two sets of three different polypeptide chains ( $\text{A}\alpha$ : 610,  $\text{B}\beta$ : 461, and  $\gamma$ : 411 residues) [1] and is encoded by three genes: *FGA*, *FGB*, and *FGG*, respectively. Each chain is synthesized, assembled into a three-chain monomer ( $\text{A}\alpha$ - $\text{B}\beta$ - $\gamma$ ), and held together into a six-chain dimer ( $\text{A}\alpha$ - $\text{B}\beta$ - $\gamma$ )<sub>2</sub> by disulfide bonds in hepatocytes [2], which is then secreted into the circulation at a concentration of 1.8–3.5 g/L in plasma. The six chains are arranged into three globular nodules. The central E region contains the N-termini of all chains, while the distal D regions contain the C-termini of the  $\text{B}\beta$  ( $\beta$ -module) and  $\gamma$  ( $\gamma$ -module) chains in addition to a short segment of  $\text{A}\alpha$  chains. The C-termini of the  $\text{A}\alpha$  chains ( $\alpha$ C domains) extend briefly through the D region and fold back into coiled-

coil connectors. Coiled-coil connectors are composed of all three chains, and link the E and D nodules [3].

The conversion of fibrinogen to fibrin is the final step in the blood coagulation cascade, and is essential for hemostasis and thrombosis. During the formation of fibrin, thrombin cleaves fibrinogen, releasing fibrinopeptides A (FpA, residues 1–16) and B (FpB, residues 1–14) from the N-termini of the  $\text{A}\alpha$  and  $\text{B}\beta$  chains, respectively, and converts fibrinogen into fibrin monomers [4]. Fibrin monomers polymerize spontaneously through a two-step process. In the first step, the release of FpA exposes a new N-terminal segment, knob ‘A’, which starts with the sequence Gly-Pro-Arg-, and binds to hole ‘a’ in the  $\gamma$ -module of another fibrin molecule. These so-called “A-a” knob-hole interactions mediate the formation of double-stranded protofibrils with a half-staggered overlap between molecules in different strands [4]. Each

\* Corresponding author at: Laboratory of Clinical Chemistry and Immunology, Department of Biomedical Laboratory Sciences, School of Health Sciences, Shinshu University, 3-1-1 Asahi, Matsumoto 390-8621, Japan.

E-mail address: [nobuoku@shinshu-u.ac.jp](mailto:nobuoku@shinshu-u.ac.jp) (N. Okumura).

<https://doi.org/10.1016/j.thromres.2019.08.017>

Received 14 May 2019; Received in revised form 19 July 2019; Accepted 17 August 2019

Available online 20 August 2019

0049-3848/ © 2019 Elsevier Ltd. All rights reserved.

protofibril strand requires the so-called “D-D” interaction, which abuts the  $\gamma$  chain of two adjacent molecules [5]. In the second step, these protofibrils grow in length to a 20–25-mer oligomer and thrombin cleaves FpB, thereby exposing a new N-terminal segment, knob ‘B’, which interacts with hole ‘b’ in the  $\beta$ -module of another molecule (the so-called “B-b” knob-hole interaction) in order to promote the lateral aggregation of protofibrils [6], resulting in the formation of thicker fibers and an insoluble fibrin clot consisting of a multi-stranded and branched fiber network [7].

Up to 400 inherited fibrinogen variants causing quantitative or qualitative alterations in this molecule have been listed on the GEHT homepage [8]. Dysfibrinogenemia, which has the qualitative characteristics of reduced functional levels and normal antigenic levels of fibrinogen, is mainly caused by a heterozygous missense or one or two residue deletion mutations [8]. Although the fibrinogen  $\gamma$ -module contains many functional sites and/or structures, hole ‘a’, the “D-D” interface,  $\gamma$ - $\gamma$  cross-linking, and high affinity  $\text{Ca}^{2+}$ ,  $\alpha\text{M}/\beta 2$ -, GPIIb/IIIa-, and tissue plasminogen activator-binding sites [9,10], the function of thrombin-catalyzed fibrin polymerization in the majority of dysfibrinogenemia cases with the  $\gamma$ -module was altered; the functions of hole ‘a’ composed of  $\gamma\text{Q329}$ ,  $\gamma\text{D330}$ , and  $\gamma\text{D364}$  [11], the “D-D” interface composed of  $\gamma\text{R275}$  to  $\gamma\text{M310}$  [11], and/or the high affinity  $\text{Ca}^{2+}$ -binding site composed of  $\gamma\text{D318}$ ,  $\gamma\text{D320}$ ,  $\gamma\text{F322}$ , and  $\gamma\text{G324}$  were reduced [12]. Therefore, the dysfunctional heterozygous fibrinogens of patients (dysfibrinogenemia) are important tools for examining the normal function of the fibrinogen to fibrin conversion. In the high affinity  $\text{Ca}^{2+}$ -binding site, many fibrinogen variants have been reported as dysfibrinogenemia, hypofibrinogenemia, or hypodysfibrinogenemia [8] (Supplementary Fig. 1), and these phenotypic variations suggest that the structural integrity of this site is important not only for fibrinogen functions, but also its secretion. The heterozygous variant fibrinogens  $\gamma\text{D318Y}$  [13] and  $\gamma\Delta\text{N319D320}$  [14,15] have been reported as dysfibrinogenemia and showed markedly reduced thrombin-catalyzed fibrin polymerization. We also reported the variant fibrinogen,  $\gamma\text{D364H}$ , located in hole ‘a’, and its markedly reduced fibrin polymerization [16].

To clarify the precise function of dysfunctional fibrinogen, an examination using recombinant (homozygous) variant fibrinogen was performed. Recombinant  $\gamma\Delta\text{N319D320}$  [17] and  $\gamma\text{D318A} + \gamma\text{D320A}$  [18] showed no polymerization under the conditions of higher thrombin and/or fibrinogen concentrations. The recombinant variant fibrinogens,  $\gamma\text{D318A}$  [18],  $\gamma\text{D320A}$  [18], and  $\gamma\text{D364H}$  [19,20], showed slower, but significant thrombin-catalyzed polymerization using “B-b” interactions only. In the present study, analyses were conducted on the fibrin polymerization abilities of the recombinant variant fibrinogens  $\gamma\text{D318Y}$  and  $\gamma\text{K321E}$ , the residues of which are within the high-affinity  $\text{Ca}^{2+}$ -binding site [12], which were then compared with the recombinant variant fibrinogens,  $\gamma\Delta\text{N319D320}$  [17] and  $\gamma\text{D364H}$  [19,20], the altered fibrin polymerization mechanisms of which have been characterized in detail.

## 2. Materials and methods

### 2.1. Preparation and production of recombinant fibrinogen variants

The fibrinogen  $\gamma$  chain expression vector pMLP- $\gamma$  ( $\gamma\text{N}$ ) [21] was altered with three mutagenic primer pairs (Supplementary Table 1), and the resultant expression vectors  $\gamma\text{D318Y}$ ,  $\gamma\Delta\text{N319D320}$ , and  $\gamma\text{K321E}$  and the wild-type were co-transfected with the histidinol selection plasmid (pMSVhis) into Chinese hamster ovary (CHO) cells that expressed normal human fibrinogen A $\alpha$  and B $\beta$  chains (A $\alpha$ B $\beta$ -CHO cells), as described previously [22]. Nine to 11 clones of fibrinogen variant-producing CHO cells were selected by measuring fibrinogen concentrations in culture media with enzyme-linked immunosorbent assays (ELISA) using a goat anti-human fibrinogen capture antibody (Cappel, Durham NC, USA) and peroxidase-conjugated goat anti-human fibrinogen antibody (Cappel) [23]. High  $\gamma\text{D318Y}$ ,  $\gamma\Delta\text{N319D320}$ , and

$\gamma\text{K321E}$  fibrinogen-producing CHO cells were established and cultured, conditioned media were harvested, and fibrinogens were purified, as described previously [24].  $\gamma\text{D364H}$  and wild-type fibrinogens were used as previously reported [19,20].

### 2.2. Functional analysis of thrombin- or batroxobin-catalyzed fibrin polymerization and clot observations

Fibrinopeptide release was examined and analyzed as described previously [20], with minor modifications. Briefly, after the fibrinogen solutions had been incubated with 0.05 U/mL of human  $\alpha$ -thrombin (Enzyme Research Laboratories, South Bend, MA, USA) for various periods followed by heat inactivation, supernatants including FpA and FpB were examined using high-performance liquid chromatography (HPLC) with a COSMOSIL 5C<sub>18</sub>-PAQ packed column (4.6  $\times$  150 mm; Nacalai Tesque, Kyoto, Japan).

Thrombin- or batroxobin-catalyzed fibrin polymerization was assessed in the presence or absence of  $\text{Ca}^{2+}$  ions or in the presence of the GGG, GPRP, or GHRP peptide (synthetic peptide acetate salt, purity > 97%; Sigma-Aldrich, St. Louis, MO, USA), and fibrin clottability was measured as described previously [19,20,25].

Briefly, after incubating thrombin (0.04 U/ml) and fibrinogen (0.36 mg/ml) at 37 °C for 4 h, fibrin clots or aggregates were removed by centrifugation at 13000  $\times$ g for 15 min. Fibrin monomers that were not incorporated into the pellet were confirmed based on the  $A_{280}$  of the supernatant, and clottability was calculated as  $(A_{280} \text{ at zero time} - A_{280} \text{ of the supernatant}) \div (A_{280} \text{ at zero time}) \times 100\%$ .

Clot samples for scanning electron microscopy (SEM) observations were prepared as described previously [25], with a few minor modifications. Images were taken at a magnification of 3000 $\times$  or 20,000 $\times$  with a 5-kV accelerating voltage. Fiber diameters were measured using Vernier calipers on a photograph enlarged by 300% and taken at a magnification of 20,000 $\times$ .

### 2.3. Gel filtration chromatography

Each reaction was initiated by the addition of thrombin (10  $\mu\text{L}$  at 0.5 or 5 U/mL) to fibrinogen (90  $\mu\text{L}$  at 0.20 mg/mL) in 20 mM N-[2-hydroxyethyl] piperazine-N'-[2-ethanesulfonic acid] (HEPES), pH 7.4, and 0.12 M NaCl (HBS buffer) containing 1 mM  $\text{CaCl}_2$  at an ambient temperature. At the specified time points, hirudin (1  $\mu\text{L}$  at 50 or 500 U/mL) was added to inhibit thrombin. After filtering with Millex-HV (pore size of 0.45  $\mu\text{m}$ ; Merck, Darmstadt, Germany), samples were injected onto a TSKgel G3000SW<sub>XL</sub> column (7.8  $\times$  300 mm; TOSOH, Tokyo, Japan), which has a separation range between 10 and 500 kDa. The column was equilibrated with 1/15 M phosphate-buffered saline (PBS) and fibrinogen and/or fibrin monomers were eluted under constant flow at 1.0 mL/min with monitoring at 280 nm [17]. To calculate the residual percentage of fibrinogen and/or fibrin monomers, the peak area of fibrinogen at the 0-minute reaction with thrombin was taken as 100%.

### 2.4. Protection assay for the plasmin digestion of fibrinogen and factor (F) XIIIa-catalyzed cross-linking of fibrin or fibrinogen

Fibrinogen (0.30 mg/mL) in HBS buffer containing 1 or 5 mM  $\text{CaCl}_2$ , 1 or 5 mM GPRP, or 5 mM ethylene-diaminetetraacetic acid (EDTA) was incubated with plasmin (0.18 U/mL; Chromogenix AB, Molngal, Sweden) at 37 °C for 2 or 24 h. Reactions were stopped by the addition of SDS sample buffer followed by boiling for 5 min. Plasmin digests were then analyzed by 10% SDS-PAGE and stained with Coomassie brilliant blue (CBB) R-250 [25].

In order to examine the function of “D-D” interactions in protofibril formation, the FXIIIa-catalyzed cross-linking ( $\gamma$ - $\gamma$  dimer formation) of fibrin or fibrinogen was performed and analyzed as described previously [25]. The rate of cross-linking of fibrin is dependent on the

frequency of “D-D” interactions among fibrin monomers in the solution, and the rate of the cross-linking of fibrinogen in the presence of the thrombin inhibitor hirudin is dependent on the frequency of “D-D” interactions among fibrinogens in the solution.

### 2.5. Molecular modeling

We generated three-dimensional structural models of the  $\gamma$ -modules of fibrinogen variants using the PDB file 3GHG [26,27] and analyzed these models with Swiss-Pdb Viewer 4.1.0 [28].

### 2.6. Statistical analysis

The significance of differences between wild-type fibrinogen and fibrinogen variants was assessed using the Student's *t*-test, a one-way ANOVA (analysis of variance), and the Turkey-Kramer test. A difference was considered to be significant when  $p < 0.05$ .

## 3. Results

### 3.1. Synthesis and secretion of recombinant fibrinogen variants in CHO cells

Wild-type fibrinogen and variants were expressed in CHO cells, cloned, and established, and fibrinogen concentrations in culture media and cell lysates were measured (Supplementary Fig. 2). Wild-type fibrinogen-producing cells had fibrinogen concentrations of  $1.35 \pm 0.12 \mu\text{g}/\text{mL}$  (mean  $\pm$  SD,  $n = 10$ ) in culture media and  $1.04 \pm 0.15 \mu\text{g}/\text{mL}$  in cell lysates, and the fibrinogen concentration ratio of culture media/cell lysates was  $1.30 \pm 0.19$ . The ratios of  $\gamma\text{D318Y}$  ( $0.70 \pm 0.17$ ,  $n = 9$ ) and  $\gamma\Delta\text{N319D320}$  fibrinogen-producing CHO cell lines ( $0.66 \pm 0.18$ ,  $n = 11$ ) were lower, while that of the  $\gamma\text{K321E}$  fibrinogen-producing CHO cell line ( $1.62 \pm 0.70$ ,  $n = 10$ ) was higher than that of the wild-type fibrinogen-producing CHO cell line.

### 3.2. FpA and FpB release, fibrin polymerization, clottability, and SEM observations

The rate of FpA release from all fibrinogen variants was not significantly different from that of wild-type fibrinogen (Fig. 1A). On the other hand, the rate of FpB release from  $\gamma\text{D318Y}$ ,  $\gamma\Delta\text{N319D320}$ , and

$\gamma\text{D364H}$  fibrinogen was slightly slower than that from the others (Fig. 1B).

Representative curves of triplicate thrombin-catalyzed fibrin polymerization are shown in Fig. 2A and Table 1.  $\gamma\text{K321E}$  fibrinogen had a slightly longer lag time ( $2.8 \pm 0.2$  min) and slightly less steep slope ( $146.9 \pm 12.3 \times 10^{-5}/\text{s}$ ) than those of wild-type fibrinogen ( $1.5 \pm 0.1$  min and  $152.2 \pm 0.0 \times 10^{-5}/\text{s}$ ). On the other hand, a turbidity change was not observed for  $\gamma\text{D318Y}$  or  $\gamma\Delta\text{N319D320}$  fibrinogen. We also examined polymerization under higher fibrinogen ( $0.45 \text{ mg}/\text{mL}$ ) conditions; however, no increase was observed in turbidity for 10 h (Fig. 2B and Table 1) or even 24 h (data not shown). Moreover, under the condition of a higher concentration of thrombin ( $1.0 \text{ U}/\text{mL}$ ), no increase in turbidity was noted for 24 h (data not shown). To compare the function of polymerization with  $\gamma\text{D318Y}$  and  $\gamma\Delta\text{N319D320}$  fibrinogens, we examined  $\gamma\text{D364H}$  fibrinogen, which showed a slower, but definite increase in turbidity after a 2-h lag period (Fig. 2B and Table 1). In the absence of  $\text{Ca}^{2+}$ , the thrombin-catalyzed polymerization of  $\gamma\text{K321E}$  fibrinogen was reduced more than in the presence of  $1 \text{ mM Ca}^{2+}$  (Fig. 2C and Table 1).

To clarify the interactions between  $\gamma\text{D318Y}$  and  $\gamma\Delta\text{N319D320}$  fibrinogens and wild-type fibrinogen, we performed thrombin-catalyzed fibrin polymerization on 1:1 mixtures of wild-type and  $\gamma\text{D318Y}$  or  $\gamma\Delta\text{N319D320}$  fibrinogens and conducted comparisons using 2:0 and 1:0 mixtures. The turbidity changes observed for the wild-type and both variant 1:1 mixtures were similar to those for the 1:0 mixture (Supplementary Fig. 3).

As shown in Fig. 2D, in the presence of the catalyst batroxobin, which releases FpA, but not FpB from fibrinogen, the fibrin polymerization of  $\gamma\text{K321E}$  fibrinogen had a longer lag time ( $9.2 \pm 0.7$  min) and slightly less steep slope ( $50.6 \pm 8.6 \times 10^{-5}/\text{s}$ ) than those of wild-type fibrinogen ( $4.0 \pm 0.2$  min and  $55.5 \pm 3.5 \times 10^{-5}/\text{s}$ ) (Table 1). On the other hand, a turbidity change was not observed for  $\gamma\text{D318Y}$ ,  $\gamma\Delta\text{N319D320}$ , or  $\gamma\text{D364H}$  fibrinogen even at a higher concentration of fibrinogen and after 10-hour (Fig. 2E and Table 1) and 24-hour incubations (data not shown). To clarify the function of holes ‘a’ and ‘b’, we performed the thrombin-catalyzed fibrin polymerization of  $\gamma\text{K321E}$  fibrinogen in the presence of the synthetic peptides GPRP and GHRP, which mimic knobs ‘A’ and ‘B’, respectively, and used GGG as the control peptide. The polymerization of  $\gamma\text{K321E}$  fibrinogen was inhibited by GPRP, but not by GHRP, similar to wild-type fibrinogen (Fig. 2F and Table 1).

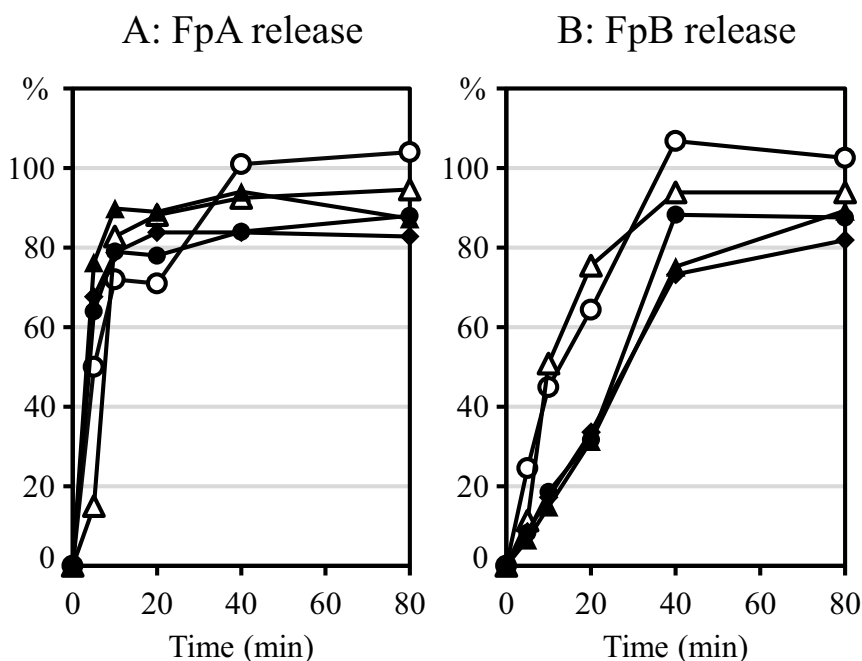
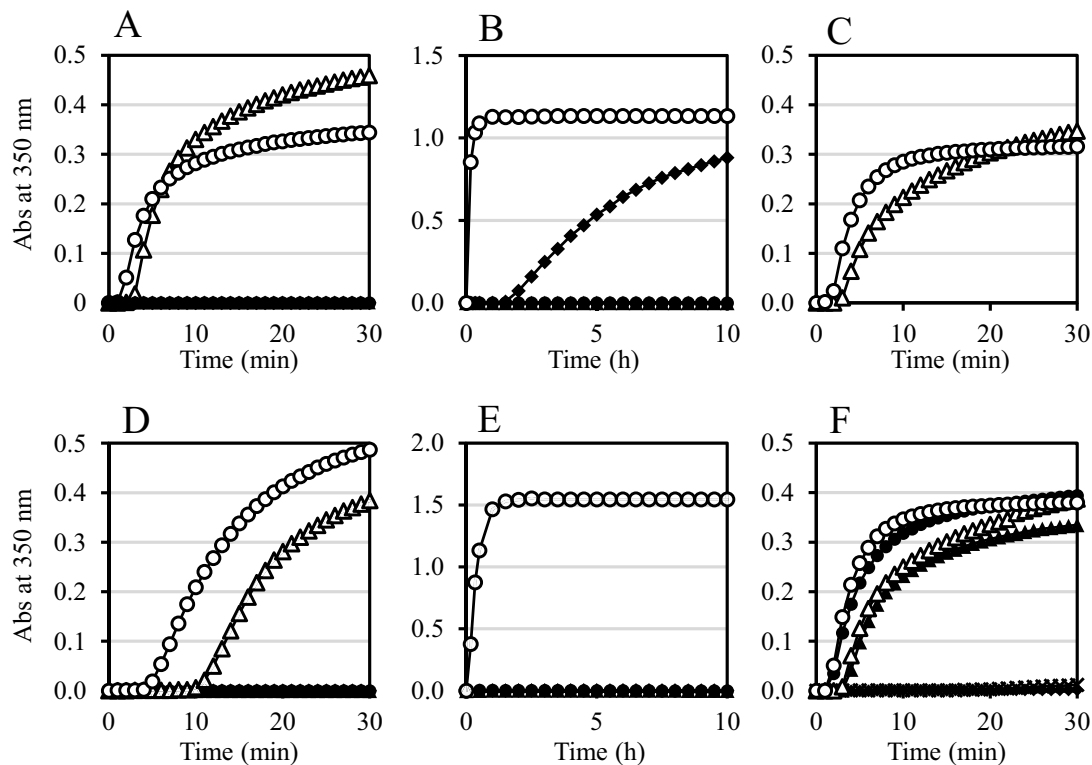


Fig. 1. Thrombin-catalyzed fibrinopeptide release. Curves of FpA (A) and FpB (B) release stimulated with thrombin ( $0.05 \text{ U}/\text{mL}$ ) were assayed by HPLC. Samples were run with wild-type ( $\circ$ ),  $\gamma\text{D318Y}$  ( $\bullet$ ),  $\gamma\Delta\text{N319D320}$  ( $\blacktriangle$ ),  $\gamma\text{K321E}$  ( $\triangle$ ), and  $\gamma\text{D364H}$  fibrinogen ( $\blacklozenge$ ) ( $0.36 \text{ mg}/\text{mL}$ ) at an ambient temperature. To calculate the percentage of the fibrinopeptide released, the amount of FpA or FpB released from each fibrinogen variant after a 2-hour incubation with  $2 \text{ U}/\text{mL}$  of thrombin at  $37^\circ\text{C}$  was taken as 100%.



**Fig. 2.** Thrombin- or batroxobin-catalyzed fibrin polymerization. Fibrin polymerization (A, C, and D: 0.18 mg/mL, B and E: 0.45 mg/mL of fibrinogen) was initiated with 0.05 U/mL thrombin (A, B, and C) or batroxobin (D and E), and the change in turbidity with time was followed at 350 nm. Polymerization was performed in the absence of Ca<sup>2+</sup> in panel C, and in the presence of 1 mM of Ca<sup>2+</sup> in the other panels. Representative turbidity curves from triplicate experiments are shown for wild-type (○), γD318Y (●), γΔN319D320 (▲), γK321E (△), and γD364H fibrinogen (◆). In panel F, 0.18 mg/mL fibrinogen (wild-type: ○, ●, or ×, γK321E: △, ▲, or ◆) was preincubated with 0.5 mM of the GGG (○ or △), GHRP (● or ▲), or GPRP (× or ◆) peptide at an ambient temperature for 1 h prior to the addition of thrombin (0.05 U/mL).

**Table 1**  
Thrombin- or Batroxobin- catalyzed fibrin polymerization.

	Thrombin			Batroxobin		
	Fibrinogen (mg/mL)	0.18	0.18	0.45	0.18	0.45
	Ca <sup>2+</sup> (mM)	0.0	1.0	1.0	1.0	1.0
wild type	Lag time (min)	1.3 ± 0.1	1.5 ± 0.1	1.3 ± 0.3	4.0 ± 0.2	4.3 ± 0.4
	Slope (x10 <sup>-5</sup> /s)	150.2 ± 14.3	152.2 ± 0.0	305.7 ± 24.0	55.5 ± 3.5	105.6 ± 16.2
γD318Y	Lag time (min)	np	np	np	np	np
	Slope (x10 <sup>-5</sup> /s)	np	np	np	np	np
γΔN319D320	Lag time (min)	np	np	np	np	np
	Slope (x10 <sup>-5</sup> /s)	np	np	np	np	np
γK321E	Lag time (min)	3.0 ± 0.3***	2.8 ± 0.2***	-	9.2 ± 0.7***	-
	Slope (x10 <sup>-5</sup> /s)	103.3 ± 16.9*	146.9 ± 12.3**	-	50.6 ± 8.6	-
γD364H	Lag time (min)	np	np	90 ± 0***	np	np
	Slope (x10 <sup>-5</sup> /s)	np	np	0.05 ± 0.00***	np	np
	Peptide	GGG	GHRP	GPRP		
wild type	Lag time (min)	1.4 ± 0.0	1.5 ± 0.1	np		
	Slope (x10 <sup>-5</sup> /s)	135.3 ± 0.0	151.3 ± 8.2	np		
γK321E	Lag time (min)	2.7 ± 0.3	3.0 ± 0.2	np		
	Slope (x10 <sup>-5</sup> /s)	111.7 ± 12.2	103.2 ± 28.7	np		

np; not polymerized, -; no data, p\* < 0.05, p\*\* < 0.01, p\*\*\* < 0.01.

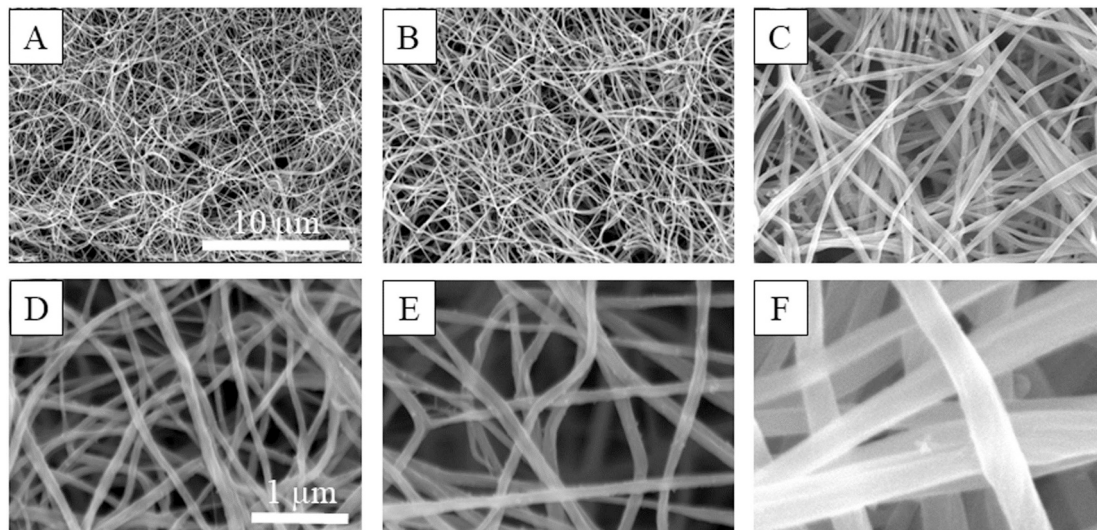


**Fig. 3.** Scanning electron microscopy of fibrin clots. Fibrinogen (0.32 mg/mL) was incubated with thrombin (0.1 U/mL) at 37 °C for 6 h. Fibrin clots were made from wild-type fibrinogen (A and D),  $\gamma$ K321E fibrinogen (B and E), or  $\gamma$ D364H fibrinogen (C and F), and recorded at a magnification of 3000 $\times$  (A, B, and C) or 20,000 $\times$  (D, E, and F). The thick white bar represents 10  $\mu$ m in panel A and 1  $\mu$ m in panel D.

To clarify whether variant fibrin monomers were incorporated into fibers, we examined clottability. The value obtained from  $\gamma$ K321E fibrinogen (91.3  $\pm$  0.5%) was not significantly different from that from wild-type fibrinogen (93.9  $\pm$  1.7%). In contrast, the values obtained from  $\gamma$ D318Y (33.6  $\pm$  4.7%) and  $\gamma$  $\Delta$ N319D320 fibrinogens (15.7  $\pm$  4.9%) were significantly lower than that from wild-type fibrinogen ( $p < 0.01$ ), whereas values from  $\gamma$ D364H fibrinogen (65.3  $\pm$  2.0%) were higher than those from  $\gamma$ D318Y and  $\gamma$  $\Delta$ N319D320 fibrinogens.

To investigate differences in the ultrastructure of fibrin clots between wild-type and  $\gamma$ K321E or  $\gamma$ D364H fibrinogen, we observed fibrin clots under SEM (Fig. 3). The fiber density of  $\gamma$ K321E fibrin clots was less than that of wild-type fibrin clots. Moreover, the fiber diameter of  $\gamma$ K321E fibrin was 114.3  $\pm$  30.6 nm ( $n = 60$ ) and thicker ( $p = 1.28 \times 10^{-10}$ ) than that of wild-type fibrin; 81.7  $\pm$  18.6 nm ( $n = 60$ ). The fiber diameter of  $\gamma$ D364H fibrin was 354.7  $\pm$  103.1 nm ( $n = 60$ ) and significantly thicker than those of wild-type fibrin ( $p = 4.33 \times 10^{-40}$ ) and  $\gamma$ K321E fibrin ( $p = 3.45 \times 10^{-34}$ ).

### 3.3. Gel filtration chromatography of fibrin monomers

We performed gel filtration chromatography to assess impairments in protofibril formation from fibrinogen variant-derived fibrin monomers (Fig. 4 and Supplementary Fig. 4). Samples were prepared as described in the Materials and Methods and run on a gel filtration column. The fibrinogen and/or fibrin monomer peak area with wild-type fibrinogen began to decrease after 5 min and residual fibrinogen and/or fibrin monomers comprised 7% at 60 min (Fig. 4A). The fibrinogen and/or fibrin monomer peak area with  $\gamma$ K321E fibrinogen also decreased after 5 min; however, its rate was slower than that of wild-type fibrinogen and residual fibrinogen and/or fibrin monomers comprised 20% at 60 min (Fig. 4B). With  $\gamma$ D318Y and  $\gamma$  $\Delta$ N319D320 fibrinogens, residual fibrinogen and/or fibrin monomers comprised 90 and 79%, respectively, at 24 h (Fig. 4C and D). On the other hand, fibrinogen and/or fibrin monomers from  $\gamma$ D364H fibrinogen began to decrease after 1 h and residual fibrinogen and/or fibrin monomers comprised 24% at 24 h, which was markedly lower than that for  $\gamma$ D318Y or  $\gamma$  $\Delta$ N319D320 fibrinogen.

### 3.4. Protection assay for the plasmin digestion of fibrinogen

To assess the functions of the high-affinity calcium binding site and

'a' hole, we performed a protection assay for plasmin digestion in the presence of CaCl<sub>2</sub> or GPRP. As shown in Fig. 5A, in the presence of 5 mM EDTA, D1-fragments derived from wild-type fibrinogen were cleaved into smaller D2- and D3-fragments, indicating no protection from plasmin digestion. On the other hand, in the presence of 1 or 5 mM CaCl<sub>2</sub> or GPRP, D1-fragments derived from wild-type fibrinogen were not cleaved into D2- or D3-fragments at 37 °C for 2 h, suggesting strong protection against plasmin digestion. However, D1-fragments were cleaved into D2-fragments under all four conditions after 24 h.

Regarding  $\gamma$ K321E fibrinogen, D1-fragments were not cleaved in a 2-hour incubation in the presence of 1 or 5 mM CaCl<sub>2</sub> or GPRP. However, in the presence of 1 mM GPRP after 24 h, D1- and D2-fragments were partially cleaved into D3- and D4-fragments, which were markedly smaller degradation products than D3-fragments (Fig. 5D). Regarding  $\gamma$ D318Y fibrinogen, in the presence of 1 or 5 mM CaCl<sub>2</sub> or GPRP, D1-fragments were all cleaved into D2- and D3-fragments in 2 h, and D1- and D2-fragments were further cleaved into D3- and D4-fragments after 24 h (Fig. 5B).

Regarding  $\gamma$  $\Delta$ N319D320 fibrinogen, in the presence of 1 or 5 mM CaCl<sub>2</sub> or GPRP in a 2-hour incubation, plasmin degradation products were similar to D1-, D2-, and D3-fragments, and were also observed in the presence of 5 mM EDTA. Moreover, these D1- and D2-fragments were further degraded into D3- and D4-fragments after 24 h (Fig. 5C).

Regarding  $\gamma$ D364H fibrinogen, D1-fragments were not cleaved in a 2-hour incubation in the presence of 1 or 5 mM CaCl<sub>2</sub>, whereas D1-fragments were partially cleaved into D2- and D3-fragments in the presence of 1 or 5 mM GPRP (Fig. 5E).

### 3.5. FXIIIa-catalyzed cross-linking of fibrin or fibrinogen

To examine the "D-D" interactions of fibrin monomers, we performed the FXIIIa-catalyzed cross-linking of  $\gamma$ -chains ( $\gamma$ - $\gamma$  dimer formation) [17], as shown in Fig. 6A–E. Fig. 6A shows that the  $\gamma$ - $\gamma$  dimer band from wild-type fibrin monomers was evident at 2 min. With a longer incubation, its intensity increased, whereas that of  $\alpha$ - and  $\gamma$ -chain bands decreased after each incubation period. With  $\gamma$ K321E fibrin monomers, the  $\gamma$ - $\gamma$  dimer band also appeared at 2 min, but its intensity was weaker than that of wild-type fibrin monomers. After a 5- to 120-min incubation, band intensities were similar to that of wild-type fibrin monomers (Fig. 6D). With  $\gamma$ D318Y and  $\gamma$  $\Delta$ N319D320 fibrin monomers, faint  $\gamma$ - $\gamma$  dimer bands appeared after 2 and 10 min, respectively; however, their intensities did not increase as clearly as that for wild-type

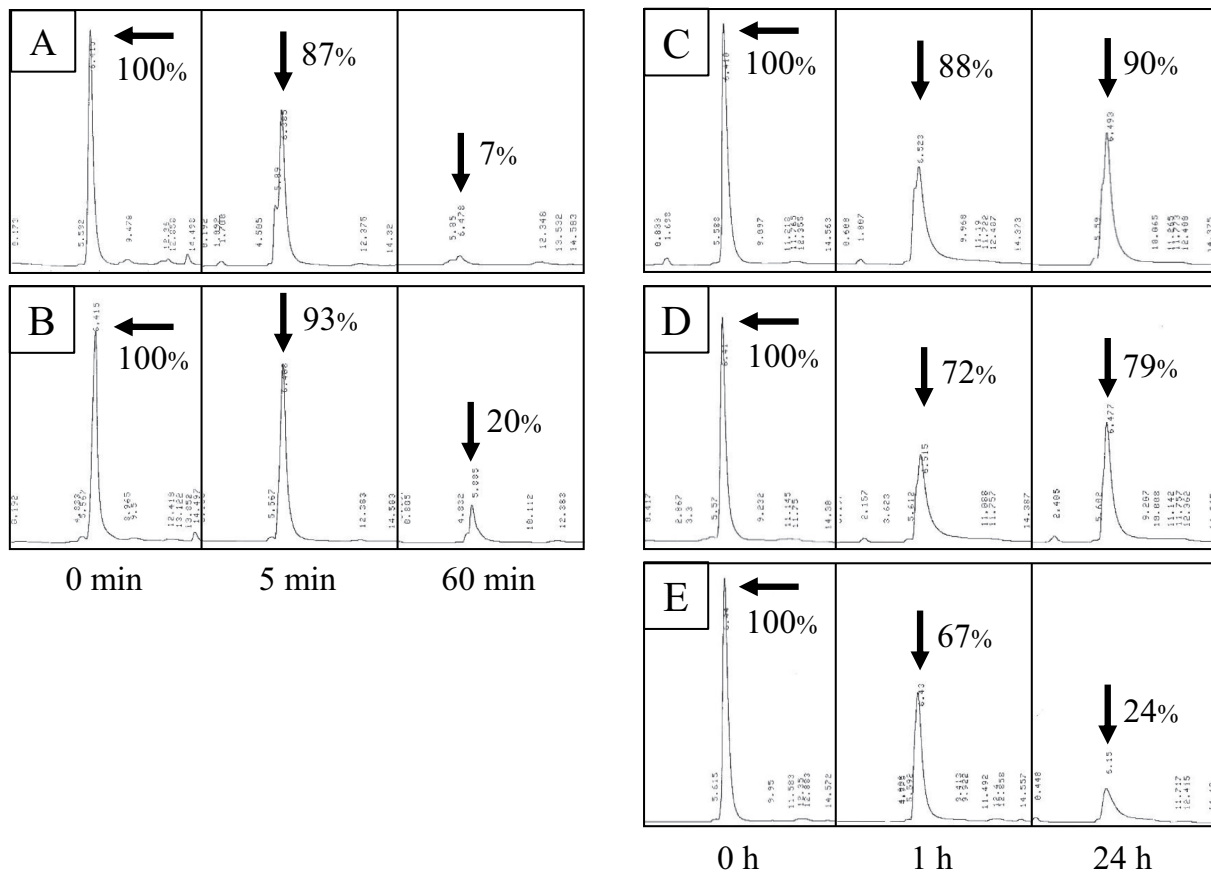


**Fig. 4.** Gel filtration chromatography. Thrombin (A, B, and E: 0.05 U/mL, C and D: 0.5 U/mL) was mixed with fibrinogen (0.18 mg/mL) and incubated at an ambient temperature. After the addition of hirudin (A, B, and E: 0.5 U/mL, C and D: 5 U/mL) to inhibit thrombin and filtering with Millex-HV (0.45 μm pore size), the sample was run over a TSKgel G3000SW<sub>XL</sub> column (7.8 × 300 mm). The peak area of fibrinogen and/or fibrin monomers was measured and the percentage of fibrinogen and/or residual fibrin monomers was calculated as described in the Materials and Methods. Panels A (wild-type) and B (γK321E) were incubated for 0, 5, or 60 min. Panels C (γD318Y), D (γΔN319D320), and E (γD364H) were incubated for 0, 1, or 24 h.

fibrin monomers after a longer incubation (Fig. 6B and C). With γD364H fibrin monomers, faint γ-γ dimer bands appeared after 2 min and gradually increased after a longer incubation (Fig. 6E).

We examined the XIIIa-catalyzed cross-linking of fibrinogen γ-chains (Fig. 6F–J). After 0.5 h, the γ-γ dimer band of wild-type fibrinogen was evident and its intensity gradually increased after a longer incubation (Fig. 6F). With γK321E fibrinogen, the γ-γ dimer band also appeared after 0.5 h; however, its intensity was weaker than that for wild-type fibrinogen (Fig. 6I). Although faint γ-γ dimer bands from γD318Y fibrinogen were present after a 0.5-hour incubation, their intensity was markedly weaker than that for wild-type fibrinogen (Fig. 6G), whereas that derived from γΔN319D320 fibrinogen was never observed (Fig. 6H). In contrast to the two variants, the γ-γ dimer bands of γD364H fibrinogen appeared after 0.5 h and gradually increased after a longer incubation, similar to wild-type fibrinogen (Fig. 6J).

### 3.6. Molecular modeling

To compare the γ-modules of γD318Y and γK321E fibrinogens with those of γD318A and γD320A fibrinogens, *in silico* analyses of their three-dimensional structures were performed and shown in Fig. 7. The degree of overall structural changes in the γD318A, γD320A, and γK321E variants was marked and similar to each other, whereas that in γD318Y was moderate relative to the normal structure.

## 4. Discussion

In the present study, we investigated the thrombin-catalyzed fibrin polymerization of recombinant γD318Y and γK321E fibrinogens mutated within the high affinity Ca<sup>2+</sup>-binding site, and compared it with the extensively studied recombinant γΔN319D320 fibrinogen mutated within the high affinity Ca<sup>2+</sup>-binding site [17], recombinant γD364H

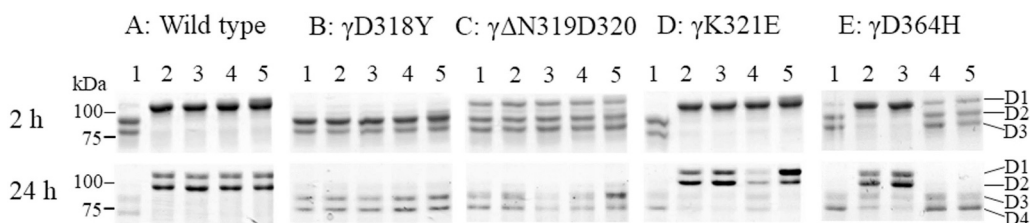


**Fig. 5.** Protection assay for the plasmin digestion of fibrinogen. Fibrinogen (0.30 mg/mL) in polymerization buffer containing 5 mM EDTA (lane 1), 1 mM EDTA (lane 2) or 5 mM CaCl<sub>2</sub> (lane 3), and 1 mM EDTA (lane 4) or 5 mM GPRP (lane 5) was incubated with 0.18 U/mL of plasmin at 37 °C for 2 or 24 h. Digests were analyzed by 10% SDS-PAGE and stained with CBB R-250. Digestion products are indicated as D1, D2, D3, and D4 on the right side of panel E.

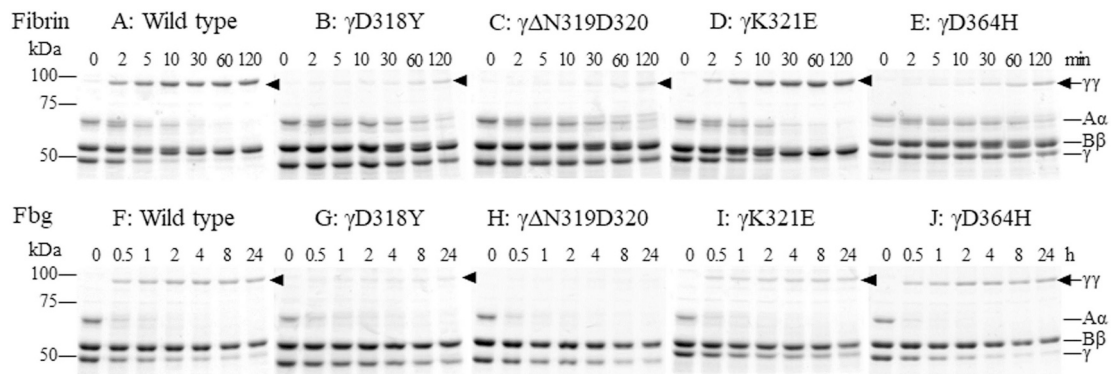


**Fig. 6.** FXIIIa-catalyzed cross-linking of fibrin or fibrinogen. The cross-linking of fibrin (A: wild-type, B:  $\gamma$ D318Y, C:  $\gamma\Delta$ N319D320, D:  $\gamma$ K321E, E:  $\gamma$ D364H) or fibrinogen (F: wild-type, G:  $\gamma$ D318Y, H:  $\gamma\Delta$ N319D320, I:  $\gamma$ K321E, J:  $\gamma$ D364H) by FXIIIa was examined by 8% SDS-PAGE under reducing conditions and stained with CBB R-250. Reduced fibrin or fibrinogen chains [ $\alpha\alpha$ ,  $\beta\beta$ ,  $\gamma$ , cross-linked  $\gamma\text{-}\gamma$  dimer ( $\blacktriangleleft$ )] are indicated on the right side of panels E and J.

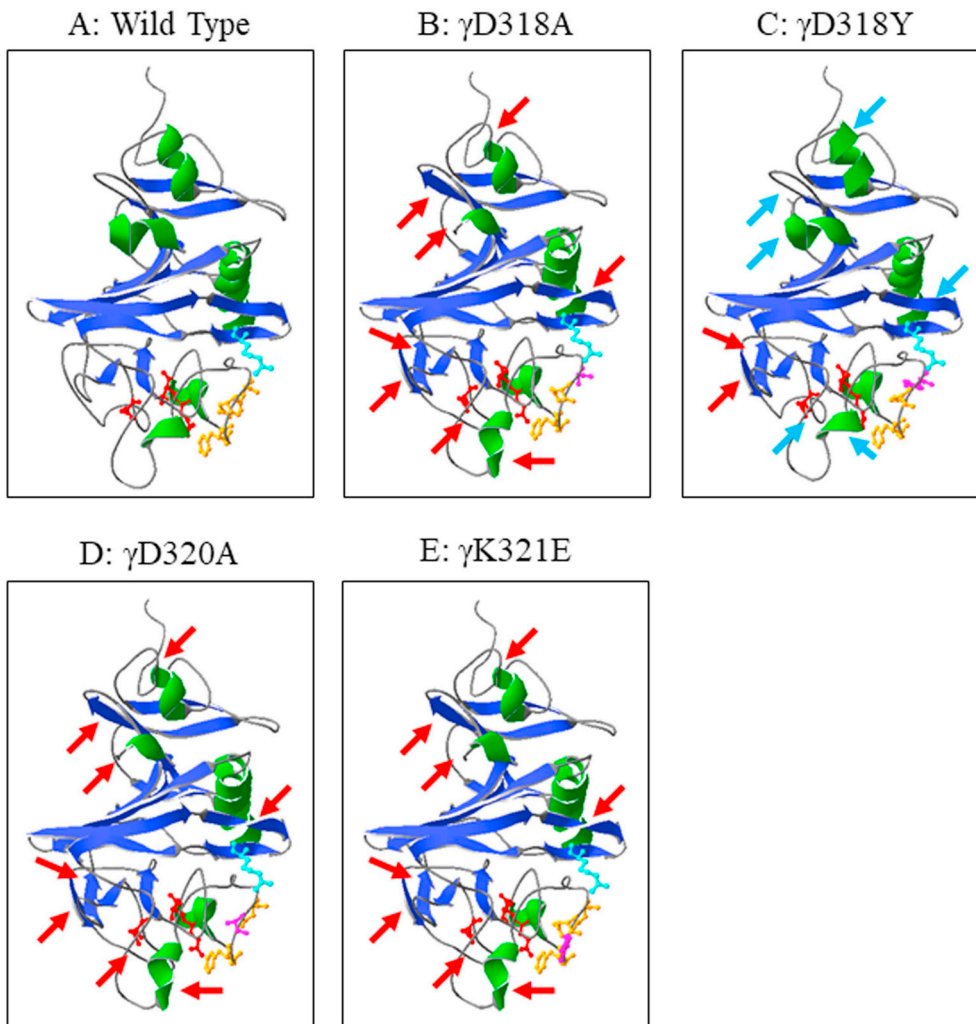


**Fig. 7.** Conformational models of normal and variant  $\gamma$ -modules. The  $\gamma$ -module three-dimensional model was prepared using PDB file 3GHG and Swiss-Pdb Viewer. Secondary structures were depicted as ribbon diagrams and indicate  $\alpha$ -helices (green) and  $\beta$ -strands (blue). Amino acids were depicted as ball-and-stick models and indicate the high affinity  $\text{Ca}^{2+}$ -binding site (orange:  $\gamma$ D318,  $\gamma$ D320,  $\gamma$ F322,  $\gamma$ G324), hole 'a' (red:  $\gamma$ Q329,  $\gamma$ D330,  $\gamma$ D364), and a part of the "D-D" interaction site (light blue:  $\gamma$ R275). In variant structures (B:  $\gamma$ D318A, C:  $\gamma$ D318Y, D:  $\gamma$ D320A, E:  $\gamma$ K321E), each altered amino acid was colored pink. Normal and aberrant secondary structures were indicated by blue and red arrows, respectively. (For interpretation of the references to colour in this figure legend, the reader is referred to the web version of this article.)

fibrinogen mutated in hole 'a', and wild-type fibrinogen [19,20]. The results obtained demonstrated that  $\gamma$ D318Y fibrinogen showed no polymerization due to the markedly reduced functions of the high affinity  $\text{Ca}^{2+}$ -binding site, hole 'a', and "D-D" interaction site. The novel recombinant variant fibrinogen  $\gamma$ K321E, for which no cases have been reported, showed only slightly reduced fibrin polymerization due to the slightly reduced function of hole 'a' and nearly normal function of the high affinity  $\text{Ca}^{2+}$ -binding site and "D-D" interaction site.

The heterozygous plasma variant fibrinogen  $\gamma\Delta$ N319D320,

Vlissingen [14] and Otsu [15], showed markedly reduced fibrin polymerization. Moreover Hogan et al. synthesized and analyzed the homozygous recombinant  $\gamma\Delta$ N319D320 fibrinogen and found no polymerization due to impaired protofibril formation with markedly reduced functions of hole 'a', the "D-D" interaction site, and the high affinity  $\text{Ca}^{2+}$ -binding site. These findings were also supported by size exclusion chromatography, transmission electron microscopic observations, and dynamic light scattering analyses [17]. On the other hand, the heterozygous plasma variant fibrinogen  $\gamma$ D318Y, Bastia [13],

showed markedly reduced fibrin polymerization and prolonged thrombin time in the absence of  $\text{Ca}^{2+}$  ions. Regarding variant fibrinogens in the high affinity  $\text{Ca}^{2+}$ -binding site, Lounes et al. [18] also reported that recombinant  $\gamma\text{D318A} + \gamma\text{D320A}$  fibrinogen showed no polymerization, whereas recombinant  $\gamma\text{D318A}$  and  $\gamma\text{D320A}$  fibrinogens showed markedly reduced fibrin polymerization. They demonstrated that the polymerization of  $\gamma\text{D318A}$  and  $\gamma\text{D320A}$  fibrinogens was supported by “B-b”, but not “A-a” interactions using the GHRP peptide, an inhibitor of “B-b” interactions as an analogue of knob ‘B’ [18]. Hogan et al. did not directly describe the mechanisms responsible for the lack of polymerization for  $\gamma\Delta\text{N319D320}$  fibrinogen [17]; however, Lounes' report [18] suggested that no polymerization of  $\gamma\Delta\text{N319D320}$  and  $\gamma\text{D318Y}$  fibrinogen was due to the lack of support by not only “A-a”, but also “B-b” interactions, similar to  $\gamma\text{D318A} + \gamma\text{D320A}$  fibrinogen. Furthermore, the markedly reduced polymerization of recombinant  $\gamma\text{D318A}$  and  $\gamma\text{D320A}$  fibrinogens was supported by “B-b” interactions only, similar to that of recombinant  $\gamma\text{D364H}$  fibrinogen, which was also inhibited of “B-b” interactions in the presence of the GHRP peptide [19,20]. Fibrinogen variants, such as  $\gamma\text{D318A}$ ,  $\gamma\text{D320A}$ , and  $\gamma\text{D364H}$ , for which hole ‘a’ is lost or severely impaired “A-a” interactions are compromised, showed impaired, but significant thrombin-catalyzed polymerization and fibrin clot formation by “B-b” interactions alone.

The present results indicated that impairments in fibrin polymerizations markedly differed between  $\gamma\text{D318A}$  and  $\gamma\text{D318Y}$  fibrinogens, and between  $\gamma\text{D320A}$  and  $\gamma\text{K321E}$  fibrinogens. Therefore, to compare structural changes in fibrinogen variants, we performed *in silico* analyses of the fibrinogen  $\gamma$ -module. The impact of overall structural changes in the  $\gamma$ -modules of the modeled variants was discordant with the results of fibrin polymerization. Although secondary structures as ribbon diagrams in Fig. 7 indicated differences among fibrinogen variants,  $\gamma\text{D318Y}$  (Fig. 7C) had markedly fewer aberrant structures, such as  $\alpha$ -helices near the  $\text{Ca}^{2+}$ -binding site and random coils near hole ‘a’, than those of  $\gamma\text{D318A}$  (Fig. 7B). This result suggests that the substitution of aspartic acid at residue 318 to tyrosine with a large aromatic side chain led to a marked structural change in the overall  $\gamma$ -module that was not predicted by Swiss-PDB Viewer, resulting in no fibrin polymerization. On the other hand,  $\gamma\text{D320A}$  (Fig. 7D) and  $\gamma\text{K321E}$  (Fig. 7E) had similar and very aberrant structures, indicating that the disappearance of the electrostatic attraction or repulsion of the negatively charged side chain of aspartic acid in  $\gamma\text{D320A}$  fibrinogen led to a severe structural change in the overall  $\gamma$ -module. Despite Swiss-PDF Viewer does not predict extreme structural changes,  $\gamma\text{D320A}$  fibrinogen showed markedly reduced fibrin polymerization more than  $\gamma\text{K321E}$  fibrinogen.

It currently remains unclear why  $\gamma\text{D318Y}$ ,  $\gamma\text{D318A} + \gamma\text{D320A}$ , and  $\gamma\Delta\text{N319D320}$  fibrinogens were not polymerized by “B-b” interactions. The latter two recombinant variant fibrinogens also showed markedly reduced platelet aggregation [17,18], which is necessary of the presence of the  $\gamma$ -chain C-terminal residues  $\gamma\text{407-411}$ . Therefore, an additional site, which was altered in these variants, appeared to be critical for platelet aggregation either alone or in the conjunction with residues  $\gamma\text{407-411}$ . These findings indicate that marked changes in the tertiary structure of the overall  $\gamma$ -module of  $\gamma\text{D318Y}$ , similar to  $\gamma\text{D318A} + \gamma\text{D320A}$  and  $\gamma\Delta\text{N319D320}$  fibrinogens, influence the location and/or orientation of the adjacent  $\beta$ -module [29], and may lead to impaired “B-b” interactions. We propose the following mechanism: the location of and/or an orientation shift in the  $\beta$ -module may change the direction of the hole ‘b’ orifice and/or elongate the distance between hole ‘b’ and knob ‘B’.

In conclusion, the recombinant fibrinogen variant,  $\gamma\text{D318Y}$ , did not polymerize due to a dysfunction in holes ‘a’ and ‘b’, which impaired protofibril formation from fibrin monomers. This result may also be applicable to  $\gamma\text{D318A} + \gamma\text{D320A}$  and  $\gamma\Delta\text{N319D320}$  fibrinogens and suggests that the altered structure in the high-affinity  $\text{Ca}^{2+}$ -binding site located in the  $\gamma$ -module and the following marked change in the tertiary structure in the whole  $\gamma$ -module influence not only hole ‘a’ and the “D”

interaction site, but also the location of and/or an orientation shift in the  $\gamma$ -module, leading to impaired “B-b” interactions. In contrast to our prediction,  $\gamma\text{K321E}$  fibrinogen exhibited only slightly impaired fibrin polymerization. The present results also demonstrated that the degree of structural changes and fibrin polymerization ability markedly varied among the variants, and may be dependent on the characterization of 1) the wild-type residue and/or 2) the substituted residue.

## Authorship

T Kamijo performed the research, analyzed the data, and wrote the manuscript. S Mukai established the fibrinogen variant-producing CHO cell lines. C Taira, Y Higuchi, and N Okumura designed the research and discussed the data, and N Okumura reviewed the manuscript.

## Declaration of competing interest

The authors have no conflicts of interest to declare.

## Acknowledgments

This work was supported by JSPS KAKENHI Grant Number JP17K09009 (C Taira and N Okumura).

## Appendix A. Supplementary data

Supplementary data to this article can be found online at <https://doi.org/10.1016/j.thromres.2019.08.017>.

## References

- [1] J.W. Weisel, Fibrinogen and fibrin, *Adv. Protein Chem.* 70 (2005) 247–299.
- [2] S. Huang, Z. Cao, D.W. Chung, E.W. Davie, The role of  $\beta\gamma$  and  $\alpha\gamma$  complexes in the assembly of human fibrinogen, *J. Biol. Chem.* 271 (1996) 27942–27947.
- [3] L. Medved, J.W. Weisel, Fibrinogen and factor XIII subcommittee of scientific standardization committee of international society on thrombosis and haemostasis, recommendations for nomenclature on fibrinogen and fibrin, *J. Thromb. Haemost.* 7 (2009) 355–359.
- [4] R.F. Doolittle, Fibrinogen and fibrin, *Annu. Rev. Biochem.* 53 (1984) 195–229.
- [5] M.W. Mosesson, K.R. Siebenlist, J.P. DiOrto, M. Matsuda, J.F. Hainfeld, J.S. Wall, The role of fibrinogen D domain intermolecular association sites in the polymerization of fibrin and fibrinogen Tokyo II ( $\gamma\text{275 Arg} \rightarrow \text{Cys}$ ), *J. Clin. Invest.* 96 (1995) 1053–1058.
- [6] Z. Yang, I. Mochalkin, R.F. Doolittle, A model of fibrin formation based on crystal structures of fibrinogen and fibrin fragments complexed with synthetic peptides, *Proc. Natl. Acad. Sci. U. S. A.* 97 (2000) 14156–14161.
- [7] M.W. Mosesson, J.P. DiOrto, K.R. Siebenlist, J.S. Wall, J.F. Hainfeld, Evidence for a second type of fibril branch point in fibrin polymer networks, the trimolecular junction, *Blood* 82 (1993) 1517–1521.
- [8] Groupe d'Etude sur l'Hémostase et la Thrombose, Base de données Des Variants du Fibrinogène. <http://site.geht.org/base-de-donnees-fibrinogene/> (accessed 15 April 2019).
- [9] M.W. Mosesson, Fibrinogen and fibrin structure and functions, *J. Thromb. Haemost.* 3 (2005) 1894–1904.
- [10] S.T. Lord, Molecular mechanisms affecting fibrin structure and stability, *Arterioscler. Thromb. Vasc. Biol.* 31 (2011) 494–499.
- [11] G. Spraggon, S.J. Everse, R.F. Doolittle, Crystal structures of fragment D from human fibrinogen and its crosslinked counterpart from fibrin, *Nature* 389 (1997) 455–462.
- [12] V.C. Yee, K.P. Pratt, H.C. Côté, I.L. Trong, D.W. Chung, E.W. Davie, et al., Crystal structure of a 30 kDa C-terminal fragment from the gamma chain of human fibrinogen, *Structure* 15 (1997) 125–138.
- [13] K.C. Lounes, C. Soria, A. Valognes, M.F. Turchini, J. Soria, J. Koopman, Fibrinogen Bastia ( $\gamma\text{318 Asp} \rightarrow \text{Tyr}$ ) a novel abnormal fibrinogen characterized by defective fibrin polymerization, *Thromb. Haemost.* 82 (1999) 1639–1643.
- [14] J. Koopman, F. Haverkate, E. Briët, S.T. Lord, A congenitally abnormal fibrinogen (Vlissingen) with a 6-base deletion in the  $\gamma$ -chain gene, causing defective calcium binding and impaired fibrin polymerization, *J. Biol. Chem.* 266 (1991) 13456–13461.
- [15] F. Terasawa, K.A. Hogan, S. Kani, M. Hirose, Y. Eguchi, Y. Noda, et al., Fibrinogen Otsu I: a gamma Asn319, Asp320 deletion dysfibrinogen identified in an asymptomatic pregnant woman, *Thromb. Haemost.* 90 (2003) 757–758.
- [16] N. Okumura, K. Furihata, F. Terasawa, R. Nakagoshi, I. Ueno, T. Katsuyama, Fibrinogen Matsumoto I: a  $\gamma\text{364Asp} \rightarrow \text{His}$  (GAT  $\rightarrow$  CAT) substitution associated with defective fibrin polymerization, *Thromb. Haemost.* 75 (1996) 887–891.
- [17] K.A. Hogan, O.V. Gorkun, K.C. Lounes, A.I. Coates, J.W. Weisel, R.R. Hantgan,

- et al., Recombinant fibrinogen Vlissingen/Frankfurt IV. The deletion of residues 319 and 320 from the  $\gamma$  chain of fibrinogen alters calcium binding, fibrin polymerization, cross-linking, and platelet aggregation, *J. Biol. Chem.* 275 (2000) 17778–17785.
- [18] K.C. Lounes, L. Ping, O.V. Gorkun, S.T. Lord, Analysis of engineered fibrinogen variants suggests that an additional site mediates platelet aggregation and that “B-b” interactions have a role in protofibril formation, *Biochemistry* 41 (2002) 5291–5299.
- [19] N. Okumura, F. Terasawa, A. Haneishi, N. Fujihara, M. Hirota-Kawadobora, K. Yamauchi, et al., B:b interactions are essential for polymerization of variant fibrinogens with impaired holes ‘a’, *J. Thromb. Haemost.* 5 (2007) 2352–2359.
- [20] K. Soya, F. Terasawa, N. Okumura, Fibrinopeptide A release is necessary for effective B:b interactions in polymerisation of variant fibrinogens with impaired A:a interactions, *Thromb. Haemost.* 109 (2013) 221–228.
- [21] M.M. Rooney, L.V. Parise, S.T. Lord, Dissecting clot retraction and platelet aggregation. Clot retraction does not require an intact fibrinogen  $\gamma$  chain C terminus, *J. Biol. Chem.* 271 (1996) 8553–8555.
- [22] S. Mukai, M. Ikeda, Y. Takezawa, M. Sugano, T. Honda, N. Okumura, Differences in the function and secretion of congenital aberrant fibrinogenemia between heterozygous  $\gamma$ D320G (Okayama II) and  $\gamma\Delta$ N319-AD320 (Otsu I), *Thromb. Res.* 136 (2015) 1318–1324.
- [23] C.G. Binnie, J.M. Hettasch, E. Strickland, S.T. Lord, Characterization of purified recombinant fibrinogen: partial phosphorylation of fibrinopeptide A, *Biochemistry* 32 (1993) 107–113.
- [24] T. Kobayashi, S. Arai, N. Ogiwara, Y. Takezawa, M. Nanya, F. Terasawa, et al.,  $\gamma$ 375W fibrinogen-synthesizing CHO cells indicate the accumulation of variant fibrinogen within endoplasmic reticulum, *Thromb. Res.* 133 (2014) 101–107.
- [25] M. Ikeda, T. Kobayashi, S. Arai, S. Mukai, Y. Takezawa, F. Terasawa, et al., Recombinant  $\gamma$ T305A fibrinogen indicates severely impaired fibrin polymerization due to the aberrant function of hole ‘a’ and calcium binding sites, *Thromb. Res.* 134 (2014) 518–525.
- [26] RCSB Protein Data Bank. <https://www.rcsb.org/> (accessed 15 April 2019).
- [27] J.M. Kollman, L. Pandi, M.R. Sawaya, M. Riley, R.F. Doolittle, Crystal structure of human fibrinogen, *Biochemistry* 48 (2009) 3877–3886.
- [28] Deep View Swiss-Pdb Viewer. <https://spdbv.vital-it.ch/> (accessed 15 April 2019).
- [29] S.J. Everse, G. Spraggon, L. Veerapandian, M. Riley, R.F. Doolittle, Crystal structure of fragment double-D from human fibrin with two different bound ligands, *Biochemistry* 37 (1998) 8637–8642.